

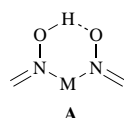
Synthesis and structure of bis(azooximates) of dichlororhodium(III): the oxime–oximate O–H···O bridge and the effect of its deprotonation

Sanjib Ganguly, Vadivelu Manivannan and Animesh Chakravorty*

Department of Inorganic Chemistry, Indian Association for the Cultivation of Science, Calcutta 700 032, India

The reaction of azooximes $\text{RC}(\text{NOH})\text{NNPh}$ ($\text{R} = \text{Me}$ HL^1 , Ph HL^2 , or $\text{C}_6\text{H}_4\text{Me-}p$ HL^3) with $\text{RhCl}_3 \cdot 3\text{H}_2\text{O}$ afforded red *trans-cis-cis*(*tcc*)- $[\text{RhCl}_2\text{L}(\text{HL})]$ **1** which was converted into green $[\text{NEt}_3\text{H}][\text{tcc-RhCl}_2\text{L}_2]$ **2** upon treatment with Et_3N ; **2** isomerises to pink $[\text{NEt}_3\text{H}][\text{cct-RhCl}_2\text{L}_2]$ **3** spontaneously in boiling benzene–toluene. The distorted octahedral co-ordination spheres are of type $\text{RhCl}_2\text{N}^{\text{o}}_2\text{N}^{\text{a}}_2$ ($\text{N}^{\text{o}} = \text{oximate N}$, $\text{N}^{\text{a}} = \text{azo N}$) with the relative arrangement of donor atom pairs as stated (e.g. *tcc* = *trans*- Cl_2 -*cis*- N^{o}_2 -*cis*- N^{a}_2). The crystal structures of *tcc*- $[\text{RhCl}_2\text{L}^2(\text{HL}^2)]$ **1b**, $[\text{NEt}_3\text{H}][\text{tcc-RhCl}_2\text{L}^2_2]$ **2b** and $[\text{NEt}_3\text{H}][\text{cct-RhCl}_2\text{L}^3_2]$ **3c** were determined. In **1b** unsymmetrical hydrogen bonding is present, the $\text{O} \cdots \text{O}$ distance being 2.515(5) Å. Upon deprotonation to **2b** the distance increases to 2.833(8) Å. In **3c** the distance is 4.207(10) Å. The NEt_3H^+ cations in **2b** and **3c** are associated with oximate oxygen and *cis*- RhCl_2 chloride respectively. The isomerisation of **2b** to **3b** in hot toluene is characterised by a high enthalpy and entropy of activation.

The hydrogen-bonded $\text{M}(\text{oxime})(\text{oximate})$ chelate motif **A**, first observed among dioxime complexes,^{1–3} has been of interest in inorganic research as a tool for building planar equatorial ligation buttressed by hydrogen bonding,^{4,5} the axial positions as well as the metal oxidation state remaining available for chemical manipulation as in cobalamine modelling⁶ and metal–metal binding.^{7,8} We have recently examined the effect of variable metal valence on the dimensions and bonding in and around **A** in a case having $\text{M} = \text{Ru}$.⁹ The present work was undertaken with the objective of scrutinising the stereochemical consequences of removing the bridge proton of **A** away to another acceptor. To our knowledge this fundamental issue has not been addressed for any case on the basis of systematic isolation and structural studies.



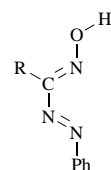
Dichlororhodium(III) bis(chelated) by arylazooximes in the *trans*- RhCl_2N_4 co-ordination mode has been found to be a good model for the present study. Under mild basic conditions bridge-proton dissociation occurs without any change in gross co-ordination geometry but with some subtle alterations of bond parameters. The system so produced is however metastable and undergoes geometrical isomerisation to a *cis*- RhCl_2N_4 complex upon heating. To our knowledge this is the first demonstration of such isomerisation promoted by the removal of the hydrogen bridge. Three groups of compounds have been characterised and the structure of one member of each type determined. The isomerisation rate has been studied in one case.

Results and Discussion

Syntheses

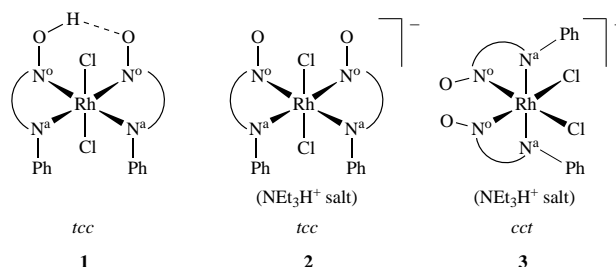
Trivalent rhodium was chosen as the metal site because of its documented ability^{10–12} to form the chelate type **A**. Further, structural changes in its co-ordination sphere are expected to be relatively slow (4d⁶), facilitating isolation of the species as formed. The good affinity of trivalent rhodium for arylazo-

oximes **HL** has been known for some years in the form of tris(chelates)¹³ and recently the moiety **A** was shown to be present in certain arylazooximates of platinum⁸ and ruthenium.⁹ This prompted us to undertake the synthesis of rhodium arylazooximates having the hydrogen-bonded chelate ring **A**.



HL^1 $\text{R} = \text{Me}$
 HL^2 $\text{R} = \text{Ph}$
 HL^3 $\text{R} = \text{C}_6\text{H}_4\text{Me-}p$

The reaction of **HL** with $\text{RhCl}_3 \cdot 3\text{H}_2\text{O}$ proceeds smoothly in boiling ethanol affording the red complex $[\text{RhCl}_2\text{L}(\text{HL})]$ **1**. Upon treating **1** with triethylamine in dichloromethane solution at room temperature, facile proton transfer occurs furnishing the green salt $[\text{NEt}_3\text{H}][\text{RhCl}_2\text{L}_2]$ **2**. Acidification of **2** in dichloromethane solution by hydrogen chloride regenerates **1**. In boiling benzene or toluene **2** quantitatively isomerises to a pink form **3**. The geometrical disposition of the co-ordinated donor pairs $\text{Cl}_2\text{-N}^{\text{o}}_2\text{-N}^{\text{a}}_2$ ($\text{N}^{\text{o}} = \text{oxime N}$, $\text{N}^{\text{a}} = \text{azo N}$) as revealed by X-ray work (see below) is *trans-cis-cis* (abbreviated *tcc*) in **1** and **2** and *cis-cis-trans*(*cct*) in **3**.



All the nine complexes synthesized (Table 1) are diamagnetic (4t_g⁶). In acetonitrile solution **1** is non-conducting but **2** and **3** display electrical conductivities in the range 60–90 Ω^{–1} cm²

Table 1 Electronic spectral data^a and Rh–Cl stretching frequencies^b

Compound	UV/VIS λ/nm ($\epsilon/\text{dm}^3 \text{ mol}^{-1} \text{ cm}^{-1}$)	IR $\tilde{\nu}(\text{Rh–Cl})/\text{cm}^{-1}$
1a <i>tcc</i> -[RhCl ₂ L ¹ (HL ¹)]	530 (1980), 400 (8240), 360 (10 430)	360
1b <i>tcc</i> -[RhCl ₂ L ² (HL ²)]	545 (1540), 465 ^c (7480), 447 (8335), 410 ^c (9055), 368 (12 300)	360
1c <i>tcc</i> -[RhCl ₂ L ³ (HL ³)]	555 (3860), 475 ^c (8805), 455 (9155), 410 ^c (9685), 373 (13 790)	365
2a [NEt ₃ H][<i>tcc</i> -RhCl ₂ L ¹ ₂]	580 (3860), 460 ^c (2800), 400 (7800), 347 (11 960)	350
2b [NEt ₃ H][<i>tcc</i> -RhCl ₂ L ² ₂]	597 (2950), 470 ^c (3290), 415 (6840), 350 (11 300)	350
2c [NEt ₃ H][<i>tcc</i> -RhCl ₂ L ³ ₂]	600 (3420), 475 ^c (3920), 415 (7835), 350 (11 035)	350
3a [NEt ₃ H][<i>cct</i> -RhCl ₂ L ¹ ₂]	462 (7895), 350 (7060)	320, 345
3b [NEt ₃ H][<i>cct</i> -RhCl ₂ L ² ₂]	485 (8280), 355 ^c (9155)	320, 345
3c [NEt ₃ H][<i>cct</i> -RhCl ₂ L ³ ₂]	505 (8270), 358 ^c (9410)	322, 348

^a In dichloromethane solution for complexes of type **1** and **3** and in acetonitrile solution for **2**. ^b As KBr disc. ^c Shoulder.

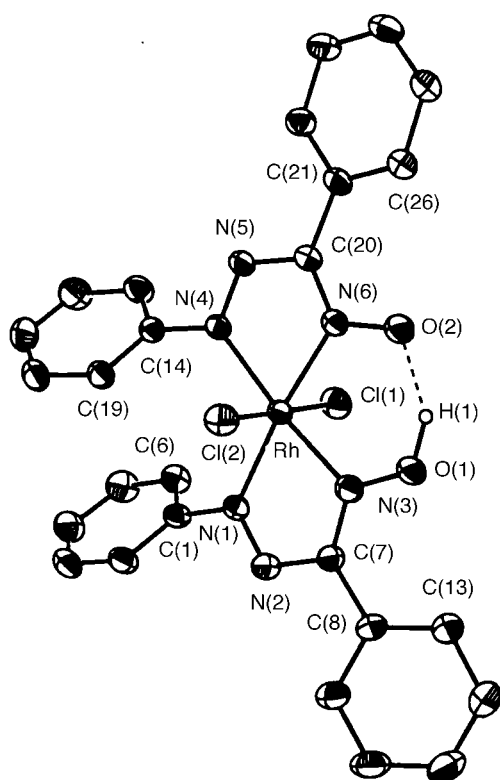


Fig. 1 An ORTEP¹⁶ plot for *tcc*-[RhCl₂L²(HL²)] **1b**. All non-hydrogen atoms are represented by their 30% probability ellipsoids

mol⁻¹ which fall below the expected 1:1 electrolyte value suggesting the presence of significant cation association.¹⁴ The X-ray structural results, described below, provide clues to the possible mode of the association.

Selected spectral data are listed in Table 1. Complexes of types **1** and **2** display a sharp single Rh–Cl stretch in the region 350–365 cm⁻¹ consistent with *trans*-RhCl₂ geometry. On the other hand, **3** having the *cis*-RhCl₂ moiety shows the two expected stretches at ≈ 320 and ≈ 345 cm⁻¹.¹⁵ In the visible region the complexes display characteristic bands: **1**, ≈ 550 ; **2**, ≈ 600 and **3**, ≈ 500 nm. The bands of **2** and **3** are useful for isomerisation studies, see below.

Structures

The crystal structures of *tcc*-[RhCl₂L²(HL²)] **1b**, [NEt₃H][*tcc*-RhCl₂L²₂] **2b** and [NEt₃H][*cct*-RhCl₂L³₂] **3c** have been determined. Molecular views are depicted in Figs. 1–3 and selected bond parameters are listed in Table 2. The co-ordination geometries are distorted octahedral and the five-membered chelate rings (oximate oxygen included) in all the three complexes as well as the six-membered chelate ring in **1b** are closely planar (mean deviation < 0.03 Å).

In both complexes **1b** and **2b** the RhCl₂ fragment is nearly

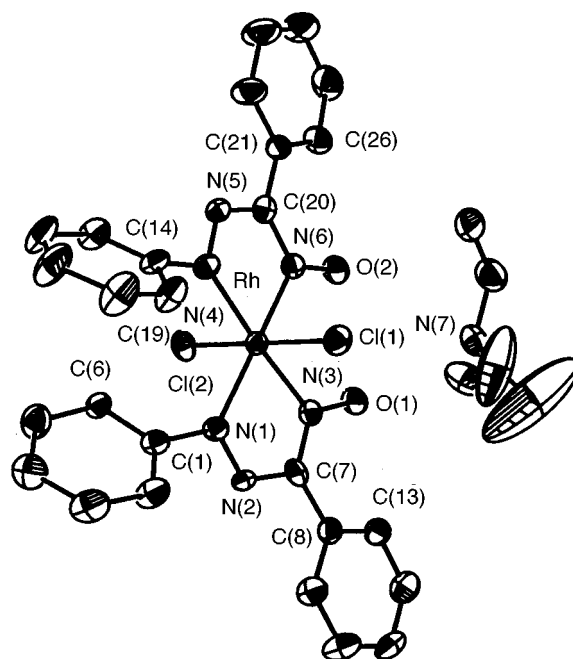


Fig. 2 An ORTEP plot for [NEt₃H][*tcc*-RhCl₂L²₂] **2b**. Details as in Fig. 1

linear, the angle at the metal centre being $\approx 178^\circ$. In **3c** the corresponding angle is $89.9(1)^\circ$. The Rh–Cl lengths in **1b** and **2b** lie within ± 0.01 Å of 2.33 Å which compares well with those in other oximate complexes incorporating the *trans*-RhCl₂ moiety.^{10,11} In **3c**, however, the average Rh–Cl bond is significantly longer, 2.391(2) Å. The *trans* influence of the oximate-N atom⁹ and the presence of N–H \cdots Cl hydrogen bonding (see below) are believed to be the main reasons for this. The average Rh–N^o length is generally shorter than the average Rh–N^a. This difference is more conspicuous in **1b** and **2b** probably because the Rh–N^a bond is subject to the *trans* influence of the Rh–N^o bond in these cases.

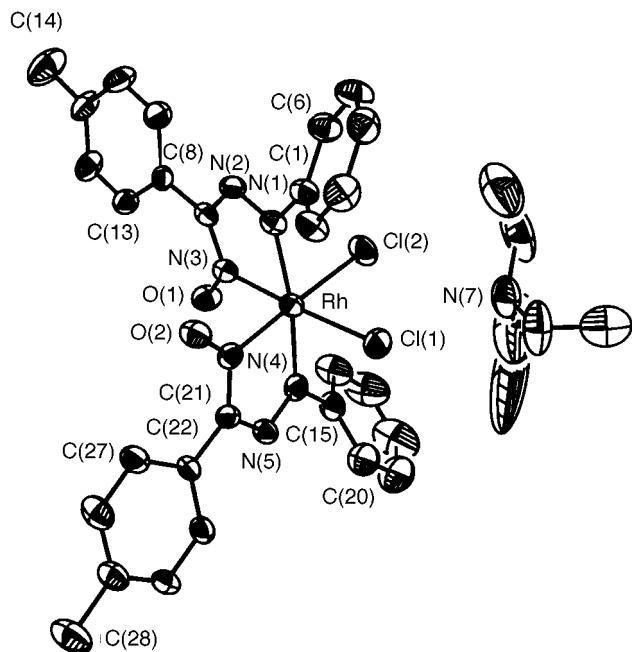
In complex **2b** the distances of the NEt₃H⁺ nitrogen from the oximate oxygen atoms are N(7) \cdots O(1) 2.848(9) and N(7) \cdots O(2) 3.297(9) Å. The former is shorter than the sum (3.1 Å) of the van der Waals radii,^{17a} suggesting N–H \cdots O association. In **3c** the NEt₃H⁺ cation is located in the sterically unencumbered vicinity of the *cis*-RhCl₂ fragment, the N(7) \cdots Cl(1) and N(7) \cdots Cl(2) distances being 3.330(7) and 3.422(7) Å respectively. The presence of weak N(7)–H \cdots Cl(1) hydrogen bonding^{17b} is indicated (sum of van der Waals radii 3.4 Å^{17a}).

The O–H \cdots O bridge in complex **1b** and the effect of proton dissociation

In complex **1b** all the hydrogen atoms including the crucial oxime H atom were directly observable in Fourier maps. The

Table 2 Selected bond lengths (Å) and angles (°) for complexes **1b**, **2b** and **3c**

	1b	2b	3c
Rh–Cl(1)	2.322(2)	2.345(2)	2.389(2)
Rh–Cl(2)	2.338(2)	2.326(2)	2.392(2)
Rh–N(1)	2.046(3)	2.064(6)	2.008(6)
Rh–N(4)	2.043(3)	2.031(6)	2.018(6)
Rh–N(3)	1.983(4)	2.032(7)	1.984(6)
Rh–N(6)	1.985(3)	2.002(6)	1.986(6)
N(3)–O(1)	1.316(5)	1.261(8)	1.254(8)
N(6)–O(2)	1.318(5)	1.273(8)	1.257(8)
O(1)···O(2)	2.515(5)	2.833(8)	4.207(10)
Cl(1)–Rh–Cl(2)	177.9(1)	178.6(1)	89.9(1)
N(1)–Rh–N(3)	75.7(1)	76.3(2)	77.7(2)
N(4)–Rh–N(6)	75.6(1)	76.2(3)	77.8(2)
N(1)–Rh–N(4)	110.9(1)	107.1(3)	171.3(2)
N(3)–Rh–N(6)	97.9(2)	100.5(2)	91.6(2)
Cl(1)–Rh–N(1)	90.6(1)	91.8(2)	90.6(2)
Cl(1)–Rh–N(3)	91.8(1)	87.1(2)	177.0(2)
Cl(1)–Rh–N(4)	89.5(1)	90.6(2)	85.8(2)
Cl(1)–Rh–N(6)	87.7(1)	92.8(2)	89.9(2)
Cl(2)–Rh–N(1)	91.1(1)	88.9(2)	86.8(2)
Cl(2)–Rh–N(3)	87.4(1)	92.0(2)	88.7(2)
Cl(2)–Rh–N(4)	91.0(1)	90.2(2)	100.1(2)
Cl(2)–Rh–N(6)	90.5(1)	86.3(2)	177.9(2)
N(1)–Rh–N(6)	173.4(2)	174.2(2)	95.3(2)
N(3)–Rh–N(4)	173.3(1)	175.9(3)	97.1(2)

**Fig. 3** An ORTEP plot for [NEt₃H][cct-RhCl₂L₂] **3c**. Details as in Fig. 1.

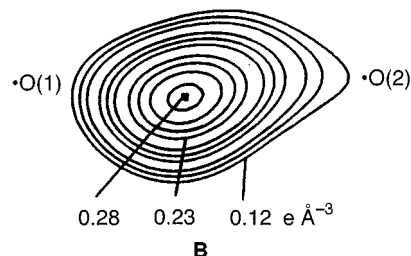
oxime H was refined isotropically affording the parameters O(1)–H(1) 1.02(4), H(1)···O(2) 1.51(4), O(1)···O(2) 2.515(5) Å and O(1)–H(1)···O(2) 146.9(5)°. The hydrogen bonding is thus unsymmetrical^{10,11} which is also evident in the difference electron-density map of **1b** in the O(1)···O(2) region viewed down the RhCl₂ axis as depicted in **B**. The density is highest near O(1) [the O(1)–H(1) bond] but it extends in the direction of O(2) representing the weaker H(1)···O(2) interaction.

Between complexes **1b** and **2b** a number of subtle structural adjustments take place. These include the increase in angles N^o–Rh–N^o, Rh–N^o–O and Rh–N^a–C by ≈3° in each case and the increase in Rh–N^o length by ≈0.03 Å (average). Further, the three chelate rings in **1b** are coplanar (mean deviation 0.03 Å) but in **2b** the two five-membered rings make a dihedral angle of 5.2°. The net effect is that the oxime O···O separation

Table 3 Rate constants and activation parameters for the isomerisation process **2b** → **3b**

<i>T</i> /K	10 ⁵ <i>K</i> /s ^{−1}	<i>T</i> /K	10 ⁵ <i>K</i> /s ^{−1}
348	0.93	368	80.33
353	3.66	373	219.01
358	8.83	378	520.29
363	28.50		

$\Delta H^\ddagger/\text{kJ mol}^{-1} = 230.12$ (23.0), $\Delta S^\ddagger/\text{kJ K}^{-1} \text{mol}^{-1} = 317.15$ (29.3)



increases by 0.3 Å on going from 2.515(5) Å in **1b** to 2.833(8) Å in **2b**. The presence of the NEt₃H⁺ cation in the vicinity (as noted above) provides some stabilisation and the O···O separation in **2b** still lies below the sum (3.0 Å) of the van der Waals radii^{17a} of two oxygen atoms. Along with the increase in O···O separation, the distance between the centre of gravity (c.g.) of the two N^a–Ph rings also increases from 3.738(6) Å in **1b** to 3.833(8) Å in **2b**.

Isomerisation

In spite of the augmented O···O separation, complex **2b** is still metastable and undergoes facile thermal isomerisation in solution to achieve larger O···O and c.g.···c.g. separations. In **3c** the two chelate rings make a dihedral angle of 93.6° and thus the oximate oxygen atoms lie on nearly orthogonal planes and their separation becomes 4.207(10) Å. The N^a–Ph rings are located in *trans* positions with a c.g.···c.g. separation of 8.418(10) Å.

The variable-temperature rates of the reaction **2b** → **3b** have been spectrophotometrically determined in toluene (348–378 K). Good isosbestic points, Fig. 4, indicate the presence of only two species. The reaction is first order in nature. Rate and activation parameters are collected in Table 3. The X-ray work has provided a clue to the nature of the cation–anion association which persists even in acetonitrile solution (conductivity data, see above). In toluene, the association is expected to be even stronger. The isomerisation could proceed by a twist pathway which is usually associated with a negative entropy of activation.¹⁸ The large and positive entropy of activation in the present system may be due to ion-pair dissociation being crucial in the rate-determining step.

Other than **3**, two isomers, *cis* and *ccc* having *cis*-RhCl₂ configurations are possible in principle for [RhCl₂L₂][−]. Also possible is the isomer *ttt* with *trans*-RhCl₂ disposition. None of these has however been observed.

Conclusion

Three groups of complexes **1–3** have been synthesized and structurally characterised providing insight into the stereochemical consequences of removing the bridge in **A**. In **1** the O–H···O hydrogen bonding creates a highly planar equator consisting of three juxtaposed chelate rings. Upon deprotonation to **2**, subtle adjustments of several angles and distances take place, the net effect being a marked increase in O···O separation by 0.3 Å. Even then **2** remains metastable and undergoes spontaneous thermal isomerisation to **3**, the process being associated with large and positive enthalpy and entropy

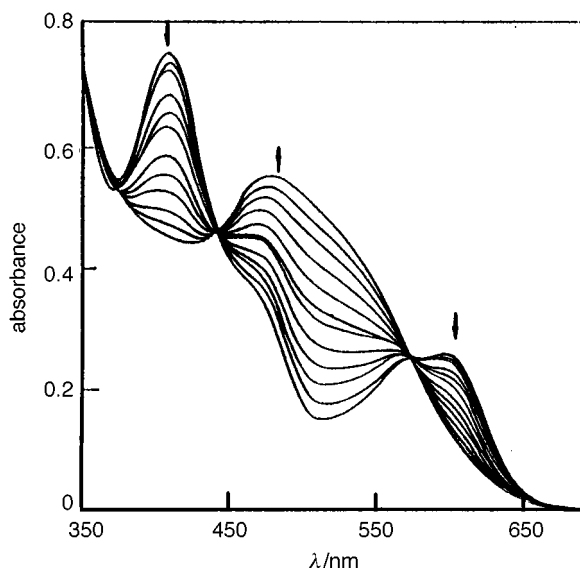


Fig. 4 Electronic spectra of an isomerising solution of $[\text{NEt}_3\text{H}][\text{tcc-RhCl}_2\text{L}_2]$ **2b** in toluene at 358 K. The arrows indicate the increase and decrease of band intensities as the reaction proceeds

of activation. This is the first example of such isomerisation resulting from oxime–oximate bridge-proton dissociation.

Experimental

Materials

Arylazooximes were prepared by reported methods¹⁹ and $\text{RhCl}_3 \cdot 3\text{H}_2\text{O}$ was obtained from Arora-Matthey, Calcutta. Toluene for rate studies was dried by distilling over sodium–benzophenone. All other chemicals were used as received.

Physical measurements

Infrared spectra were recorded with a Perkin-Elmer 783 spectrophotometer, electronic spectra with a Hitachi 330 spectrophotometer. A Perkin-Elmer 240C elemental analyser was used to collect microanalytical data (C, H, N). Conductivity measurements were carried out in acetonitrile on a Philips PR9500 bridge.

Syntheses

***tcc*-Dichloro[(phenylazo)benzaldoximate][(phenylazo)benzaldoxime]rhodium(III), *tcc*- $[\text{RhCl}_2\text{L}^2(\text{HL}^2)]$ **1b**.** The compound $\text{RhCl}_3 \cdot 3\text{H}_2\text{O}$ (0.10 g, 0.38 mmol) was dissolved in hot dry ethanol (15 cm³). To this HL^2 (0.188 g, 0.835 mmol) dissolved in the same solvent (10 cm³) was added and the mixture was heated to reflux for 10 min. The solution was then cooled to room temperature. The red crystals deposited were filtered off, washed thoroughly with ethanol and water and then dried *in vacuo* over P_4O_{10} . Yield 0.130 g (55%) (Found: C, 50.00; H, 3.45; N, 13.40. Calc. for $\text{C}_{26}\text{H}_{21}\text{Cl}_2\text{N}_6\text{O}_2\text{Rh}$: C, 50.04; H, 3.37; N, 13.47%).

The other two complexes of this family were synthesized with similar yields (Found: C, 38.49; H, 3.51; N, 16.90. Calc. for $\text{C}_{16}\text{H}_{17}\text{Cl}_2\text{N}_6\text{O}_2\text{Rh}$ **1a**: C, 38.44; H, 3.40; N, 16.82. Found: C, 51.47; H, 3.86; N, 12.81. Calc. for $\text{C}_{28}\text{H}_{24}\text{Cl}_2\text{N}_6\text{O}_2\text{Rh}$ **1c**: C, 51.57; H, 3.84; N, 12.89%).

Triethylammonium *tcc*-dichlorobis[(phenylazo)benzaldoximate]rhodate(III), $[\text{NEt}_3\text{H}][\text{tcc-RhCl}_2\text{L}^2]$ **2b.** To a solution of *tcc*- $[\text{RhCl}_2\text{L}^2(\text{HL}^2)]$ (0.1 g, 0.16 mmol) in dichloromethane (20 cm³) was added Et_3N (0.33 g, 0.33 mmol). The solution changed from red to green and was evaporated to dryness *in vacuo*. The green solid obtained was washed with hexane and dried *in vacuo*

over P_4O_{10} . Yield essentially quantitative (Found: C, 53.05; H, 4.99; N, 13.48. Calc. for $\text{C}_{32}\text{H}_{36}\text{Cl}_2\text{N}_7\text{O}_2\text{Rh}$: C, 53.00; H, 4.97; N, 13.53%).

The other two complexes of this type were prepared by similar procedures and in similar yields (Found: C, 43.87; H, 5.20; N, 16.40. Calc. for $\text{C}_{22}\text{H}_{32}\text{Cl}_2\text{N}_7\text{O}_2\text{Rh}$ **2a**: C, 43.96; H, 5.33; N, 16.32. Found: C, 54.28; H, 5.39; N, 13.12. Calc. for $\text{C}_{34}\text{H}_{40}\text{Cl}_2\text{N}_7\text{O}_2\text{Rh}$ **2c**: C, 54.22; H, 5.32; N, 13.02%).

Triethylammonium *cct*-dichlorobis[(phenylazo)benzaldoximate]rhodate(III), $[\text{NEt}_3\text{H}][\text{cct-RhCl}_2\text{L}^2]$ **3b.** A solution of $[\text{NEt}_3\text{H}][\text{tcc-RhCl}_2\text{L}^2]$ (0.1 g, 0.138 mmol) in benzene (25 cm³) was heated to reflux for 10 min, during which time it changed from green to pink. The solution was evaporated to dryness *in vacuo* and the desired complex obtained as a pink crystalline solid in nearly quantitative yield (Found: C, 52.98; H, 4.95; N, 13.58. Calc. for $\text{C}_{32}\text{H}_{36}\text{Cl}_2\text{N}_7\text{O}_2\text{Rh}$: C, 53.00; H, 4.97; N, 13.53%).

The other two complexes of this family were prepared similarly in similar yields (Found: C, 43.99; H, 5.35; N, 16.24. Calc. for $\text{C}_{22}\text{H}_{32}\text{Cl}_2\text{N}_7\text{O}_2\text{Rh}$ **3a**: C, 43.96; H, 5.33; N, 16.32. Found: C, 54.18; H, 5.32; N, 12.95. Calc. for $\text{C}_{34}\text{H}_{40}\text{Cl}_2\text{N}_7\text{O}_2\text{Rh}$ **3c**: C, 54.22; H, 5.32; N, 13.02%).

Rate measurements

Isomerisation of complex **2b** to **3b** was monitored spectrophotometrically in toluene. A solution (25 cm³) of **2b** of known concentration (5.0×10^{-4} mol dm⁻³) was taken in a three-necked flask fitted with a thermometer, a rubber septum and a water-cooled condenser. The flask was heated in an oil-bath the temperature of which could be accurately controlled. Aliquots (0.50 cm³) of solution were withdrawn *via* the rubber septum at known intervals and then cooled immediately to 298 K to halt the reaction. Each was then diluted to 5.00 cm³ and used to monitor the conversion spectrophotometrically. The absorption (A_t) at 412 nm was used. Values of the first-order rate constant k were obtained from slopes of linear least-squares plots of $-\ln(A_\infty - A_t)$ against t . A minimum of 12 data points covering three half-lives was used for each calculation. The activation parameters ΔH^\ddagger and ΔS^\ddagger were obtained from Eyring plots.²⁰

Crystallography

Single crystals of complexes **1b** (0.20 × 0.34 × 0.40 mm) and **2b** (0.26 × 0.46 × 0.50 mm) were grown by slow diffusion of hexane into dichloromethane solutions and those of **3c** (0.20 × 0.20 × 0.25 mm) by slow diffusion of hexane into acetone, followed by slow evaporation. Cell parameters were determined by least-squares fit of 30 machine-centred reflections ($2\theta = 15\text{--}30^\circ$). Systematic absences afforded the space group $P2_1/c$ for **1b** and $P2_1/n$ for **3c**; **2b** could belong either to $Pna2_1$ or $Pnma$ and successful structure solution confirmed the former. Data were collected by the ω -scan technique in the range of $3 \leq 2\theta \leq 50^\circ$ for **1b** and **2b** and of $3 \leq 2\theta \leq 45^\circ$ for **3c**. Two check reflections measured after every 98 did not show any significant change in intensity. Data were corrected for Lorentz-polarisation effects and absorption (azimuthal scans²¹). Of the 4556 (**1b**), 3057 (**2b**) and 4780 (**3c**) unique reflections, 3264, 2382 and 2667 respectively with $I > 3\sigma(I)$, $I > 2.5\sigma(I)$ and $I > 3\sigma(I)$ respectively were used for structure solution (direct method). All the non-hydrogen atoms were treated anisotropically and in the case of **1b** the oxime H was refined isotropically. All the hydrogen atoms in **2b** and **3c** were added at calculated positions with fixed U (0.08 Å²). Least-squares refinements were performed by full-matrix procedures. All calculations were done on a Micro-VAXII computer with the SHELXTL PLUS program²² and crystal structure plots were drawn using ORTEP.¹⁶ Significant crystal data are listed in Table 4.

CCDC reference number 186/794.

Table 4 Crystal data for complexes **1b**, **2b** and **3c**

	1b	2b	3c
Formula	C ₂₆ H ₂₁ Cl ₂ N ₆ O ₂ Rh	C ₃₂ H ₃₆ Cl ₂ N ₇ O ₂ Rh	C ₃₄ H ₄₀ Cl ₂ N ₇ O ₂ Rh
<i>M</i>	623.3	724.5	752.5
Crystal system	Monoclinic	Orthorhombic	Monoclinic
Space group	<i>P</i> 2 ₁ / <i>c</i>	<i>P</i> na2 ₁	<i>P</i> 2 ₁ / <i>n</i>
<i>a</i> /Å	9.387(5)	9.984(4)	10.695(3)
<i>b</i> /Å	29.247(15)	16.558(9)	27.746(12)
<i>c</i> /Å	10.268(5)	20.324(9)	12.390(5)
β/°	114.25(4)		98.03(3)
<i>U</i> /Å ³	2570(2)	3360(3)	3641(2)
<i>Z</i>	4	4	4
<i>D</i> _c /cm ⁻³	1.611	1.432	1.373
Transmission coefficients ^a	0.7333, 1	0.7289, 1	0.7789, 1
μ(Mo-Kα)/cm ⁻¹	9.09	7.07	6.55
<i>F</i> (000)	1256	1488	1552
Total number of reflections	4977	3381	5220
Number of unique reflections	4556	3057	4780
Number of observed reflections	3264	2382	2667
<i>g</i> in <i>w</i> = 1/[σ ² (<i>F</i>) + <i>g</i> <i>F</i> ²]	0.0003	0.002	0.0002
Number of refined parameters	334	396	415
<i>R</i> ^b	0.030	0.036	0.043
<i>R</i> ^c	0.037	0.046	0.044
Goodness of fit	1.27	1.10	1.45
Maximum and mean Δ/σ	0.002, 0.001	0.007, 0.001	0.006, 0.000
Data-to-parameter ratio	9.8	6.0	6.4
Maximum, minimum difference peaks/e Å ⁻³	0.34, -0.31	0.67, -0.67	0.40, -0.44

^a Maximum value normalized to 1. ^b Σ||*F*_o| - |*F*_c||/Σ|*F*_o|. ^c [Σ*w*(|*F*_o| - |*F*_c|)²/Σ*w*|*F*_o|²]^{1/2}.

Acknowledgements

Financial support from the Department of Science and Technology, Council of Scientific and Industrial Research and Indian National Science Academy, New Delhi is acknowledged. Affiliation to the Jawaharlal Nehru Centre for Advanced Scientific Research, Bangalore is also acknowledged.

References

- 1 L. Tschugaeff, *Chem. Ber.*, 1905, **38**, 2520.
- 2 L. E. Godycki and R. E. Rundle, *Acta Crystallogr.*, 1953, **6**, 487.
- 3 A. Chakravorty, *Coord. Chem. Rev.*, 1974, **13**, 1.
- 4 E. O. Schelmpfer, *Acta Crystallogr., Sect. B*, 1977, **33**, 2482.
- 5 L. F. Szczepura, J. G. Muller, C. A. Bessel, R. F. See, J. S. Janik, M. R. Churchill and K. J. Takeuchi, *Inorg. Chem.*, 1992, **31**, 859.
- 6 N. B. Pahor, M. Forcolin, L. G. Marzilli, L. Randaccio, M. F. Summers and P. J. Toscano, *Coord. Chem. Rev.*, 1985, **63**, 1; N. B. Pahor, R. Dreos-Garlatti, S. Geremia, L. Randaccio, G. Tazher and E. Zangrando, *Inorg. Chem.*, 1990, **29**, 3437.
- 7 T. W. Thomas and A. E. Underhill, *Chem. Soc. Rev.*, 1972, **1**, 99; K. G. Caulton and F. A. Cotton, *J. Am. Chem. Soc.*, 1971, **93**, 1914.
- 8 C. K. Pal, S. Chattopadhyay, C. Sinha and A. Chakravorty, *Inorg. Chem.*, 1994, **33**, 6140.
- 9 V. Manivannan, B. K. Dirghangi, C. K. Pal and A. Chakravorty, *Inorg. Chem.*, 1997, **36**, 1526.
- 10 F. Asaro, G. Pellizer, C. Tarangacco and G. Costa, *Inorg. Chem.*, 1994, **33**, 5404.
- 11 S. Siripaisarnpipat and E. O. Schlemper, *Inorg. Chem.*, 1983, **22**, 282; *J. Coord. Chem.*, 1984, **13**, 281; *Inorg. Chem.*, 1984, **23**, 330.
- 12 N. B. Pahor, R. D. Garlatti, S. Geremia, L. Randaccio, G. Tazher and E. Zangrando, *Inorg. Chem.*, 1990, **29**, 3437; M. Dunaj-Jurco, V. Kettmann, D. Steinborn and M. Ludwig, *Acta Crystallogr., Sect. C*, 1995, **51**, 210; F. A. Cotton and J. G. Norman, jun., *J. Am. Chem. Soc.*, 1971, **93**, 80.
- 13 K. C. Kalia and A. Chakravorty, *Inorg. Chem.*, 1969, **8**, 2586.
- 14 W. J. Geary, *Coord. Chem. Rev.*, 1971, **7**, 81.
- 15 G. C. Kulasingam, W. R. McWhinnie and J. D. Miller, *J. Chem. Soc. A*, 1969, 521.
- 16 C. K. Johnson, ORTEP, Report ORNL-5138, Oak Ridge National Laboratory, Oak Ridge, TN, 1976.
- 17 (a) J. E. Huheey, E. A. Keiter and R. L. Keiter, *Inorganic Chemistry: Principles of Structure and Reactivity*, Harper Collins, New York, 4th edn., 1993, p. 292; (b) F. A. Cotton and G. Wilkinson, *Advanced Inorganic Chemistry*, Wiley, Singapore, 5th edn., 1983, p. 93.
- 18 N. Serpone and D. G. Bickley, *Prog. Inorg. Chem.*, 1972, **17**, 391 and refs. therein; B. Jordan, *Reaction Mechanisms of Inorganic and Organometallic Systems*, Oxford University Press, New York, 1991, p. 94.
- 19 K. C. Kalia and A. Chakravorty, *J. Org. Chem.*, 1970, **35**, 2231.
- 20 R. C. Wilkins, *The Study of Kinetics and Mechanism of Reactions in Transition Metal Complexes*, Allyn and Bacon, Boston, 1974, p. 79.
- 21 A. C. T. North, D. C. Phillips and F. S. Mathews, *Acta Crystallogr., Sect. A*, 1968, **24**, 351.
- 22 G. M. Sheldrick, SHELXTL PLUS 88, Structure Determination Software Programs, Nicolet Instrument Corp., Madison, WI, 1988.

Received 5th August 1997; Paper 7/05690G